Neurosci. Bull. December, 2019, 35(6):959–968
https://doi.org/10.1007/s12264-019-00349-w

www.neurosci.cn
www.springer.com/12264

ORIGINAL ARTICLE

A Neuronal Pathway that Commands Deceleration in *Drosophila* Larval Light-Avoidance

Caixia Gong[1] · Zhenhuan Ouyang[2] · Weiqiao Zhao[1] · Jie Wang[1] · Kun Li[1] · Peipei Zhou[1] · Ting Zhao[3] · Nenggan Zheng[2] · Zhefeng Gong[1]

Received: 22 November 2018 / Accepted: 26 December 2018 / Published online: 27 February 2019

Abstract When facing a sudden danger or aversive condition while engaged in on-going forward motion, animals transiently slow down and make a turn to escape. The neural mechanisms underlying stimulation-induced deceleration in avoidance behavior are largely unknown. Here, we report that in *Drosophila* larvae, light-induced deceleration was commanded by a continuous neural pathway that included prothoracicotropic hormone neurons, eclosion hormone neurons, and tyrosine decarboxylase 2 motor neurons (the PET pathway). Inhibiting neurons in the PET pathway led to defects in light-avoidance due to insufficient deceleration and head casting. On the other hand, activation of PET pathway neurons specifically caused immediate deceleration in larval locomotion. Our findings reveal a neural substrate for the emergent deceleration response and provide a new understanding of the relationship between behavioral modules in animal avoidance responses.

Keywords *Drosophila* · Larva · Deceleration · Light avoidance · EH neurons · PTTH neurons · Tdc2 motor neurons

Introduction

Avoidance responses are generally thought to result from the activation of neurons that program avoidance behavior in response to external stimuli. When making an avoidance response during locomotion, animals such as *Drosophila* generally choose from two options: (1) stop on-going movement and perform a backward movement to leave [1–5], or (2) stop on-going movement, change the heading direction by making a turn, and continue forward movement to leave [6–9]. In both modes, it is necessary to stop on-going forward movement to successfully escape. Although the neural circuits for initiating or maintaining locomotion have been relatively well studied [10–14], the neural mechanisms involved in stopping behavior have received relatively little investigation. Most studies related to this topic focus only on stopping behavior – simply the cessation of movement without further action [15–18]. However, the neural mechanisms underlying the stopping or deceleration response that is followed by further behavioral maneuvers such as turning or backward movement, and their role in typical avoidance behavior, are still unclear. We hypothesized that the deceleration response is controlled by a specific neural pathway to serve as a critical initial step for avoiding danger.

Widely used in avoidance studies, phototaxis in *Drosophila* larvae is a well-suited model for testing such a hypothesis. When encountering a light area in a dark environment, a larva casts its head from side to side (i.e., sweeps its head back and forth) and then makes a turn to

Electronic supplementary material The online version of this article (https://doi.org/10.1007/s12264-019-00349-w) contains supplementary material, which is available to authorized users.

✉ Nenggan Zheng
zng@zju.edu.cn

✉ Zhefeng Gong
zfgong@zju.edu.cn

[1] Department of Neurobiology, Key Laboratory of Medical Neurobiology of the Ministry of Health of China, Key Laboratory of Neurobiology, Zhejiang University School of Medicine, Hangzhou 310058, China

[2] Qiushi Academy for Advanced Studies, Zhejiang University, Hangzhou 310007, China

[3] Janelia Research Campus, Howard Hughes Medical Institute, Ashburn, VA 22011, USA

change the direction of movement [8, 19]. Although not regularly mentioned, larvae consistently slow down prior to head casting and turning behavior [6, 20]. The neural circuitry underlying larval light avoidance has not been fully characterized. Larvae sense light either by Bolwig's organs (BOs), which are located in the anterior tip and are responsive to light of low or intermediate intensity, and multidendritic neurons in the body wall that are only sensitive to high-intensity light [21]. BOs send projections into the brain and synapse on lateral neurons, such as pigment-dispersing factor neurons and fifth lateral neurons, which are involved in phototaxis [22–24]. Prothoracicotropic hormone (PTTH) neurons, which are required for normal phototaxis, are downstream of the lateral neurons [25–27]. However, the way in which visual signals are transmitted to the motor system to generate avoidance behavior is not clear.

Therefore, we set out to determine the downstream neurons of PTTH neurons in phototaxis-regulating pathway and how the neurons in the pathway control light avoidance.

Materials and Methods

Fly Culture and Strains

All flies were raised at 25°C on standard medium in a room with a 12 h:12 h light/dark cycle. For details of fly stock sources, see Supplemental Experimental Procedures.

Behavioral Tests

In the behavioral assay for light/dark preference, 20 third-instar larvae were allowed to choose between light and dark for 10 min. In the light spot assay, individual larvae were allowed to start from darkness and enter a blue light spot on an agar plate. The whole process of larval entry and exit of the light spot was recorded and analyzed using SOS software, a computer-vision tracking system written in Matlab (Mathworks) [6] and custom-written scripts. For optogenetics and larval locomotion, larvae of the proper genotypes raised on food supplied with 5.0 mmol/L trans-retinal were stimulated with 620-nm (red) light during straight forward locomotion. Video recordings of larval locomotion were processed with SOS and custom-written software (see Supplemental Experimental Procedures for details).

Calcium Imaging and Confocal Microscopy

For Ca^{2+} imaging, individual second-instar larvae were immobilized with a coverslip. To assess responses to optogenetic stimulation, Ca^{2+}-dependent fluorescent intensity in neurons was monitored with an Olympus FV1200 MPE multi-photon microscope (Tokyo, Japan). Images were processed using Image J (https://imagej.nih.gov/ij/) (see Supplemental Experimental Procedures for details). For confocal microscopy, dissected larval brains were mounted and viewed using an Olympus FV1000 confocal laser scanning microscope.

Statistics

Statistics were performed with Prism6.0 (Graphpad Inc., https://www.graphpad.com/). For SOS-derived locomotor speed and head cast angle data, the nonparametric *Mann-Whitney* test and *Kruskal-Wallis* followed by *Dunn's post hoc* test were used. For all other data that were assumed to conform to a Gaussian distribution, we used Student's *t*-tests or ANOVA followed by *Tukey's post hoc* test.

Results

Deceleration Was Necessary for Head Casting and Light Avoidance

Because avoidance behavior typically involves changing the heading direction, we analyzed the time series of larval movement-related parameters during head casting in light-avoidance using a light-spot assay [19]. We found two interesting phenomena: (1) deceleration was almost always initiated before head casting, and (2) the head cast was initiated during deceleration. The former finding implied that deceleration is not a result of head casting, and the latter indicated that a larva does not have to fully stop to turn its head. As expected, the maximal body bending appeared after the angular velocity peak (Fig. S1A, Movie S1). As the sequential occurrence of deceleration, head casting, and maximal body bending appeared to be stereotypical, we named it the DOT pattern (deceleration starts → headomega peaks → headtheta peaks, see "Methods" for details). As shown in Figure S1B, larval locomotor speed normally dropped within 1 s before the initiation of body bending. The negative correlation between minimal speeds and maximal sizes of head casting showed that the size of the head cast tended to be greater when the speed after deceleration was lower (Fig. S1C, D). Remarkably, the size of the head cast decreased with increasing speed of movement. As a result, large head casts (>50°) only occurred at low speeds (Fig. S1C). Comparing with the case during free movement, the speed after deceleration in the light response was significantly lower and the size of the head cast following deceleration was significantly larger (Fig. S1E, F). Given that PTTH

neurons are required for larval light avoidance [25, 26, 28], we determined whether they play a role in mediating the light-induced deceleration. Larvae with blocked PTTH neurons exhibited smaller head casts when encountering light in the light-spot assay (Fig. S1G). Meanwhile, the minimal speed after light-induced deceleration was significantly higher than that in the parental controls (Fig. S1H), while the locomotor speeds in the experimental and control groups during free movement were all >1 mm/s and did not significantly differ (Fig. S2). Thus, a lack of light-avoidance may be caused by a defect in light-induced deceleration, at least in the case of inhibiting PTTH neurons.

It should be noted that the degree of head casting could be either large or small at low speed (Fig. S1C), such that it did not correspond to the speed value in a one-to-one manner. Therefore, the relationship between speed and head casting was not like the velocity-curvature relationship of a projectile as defined by physical laws, or the stereotyped velocity-curvature relationship when human or animal moves in a curved trajectory [29, 30]. There must be neural mechanisms that control the larval deceleration and head casting separately, but in a coordinated manner.

EH Neurons are Innervated by PTTH Neurons in Larval Light-Avoidance

We next determined where PTTH neurons could send output. One pair of EH-expressing neurons that are known to regulate eclosion in response to light-on at dawn [31] became candidates. We used *EH-Gal4* to drive the expression of the presynaptic marker syt-GFP [32, 33] and the postsynaptic marker Denmark [33]. The syt-GFP signal was mainly located in the corpora cardiaca of the ring gland and along the midline of the ventral nerve cord (VNC), suggesting that these regions were presynaptic sites. The Denmark signal was located mainly in the medial anterior part of each hemisphere, close to the dendrites of PTTH neurons (Fig. 1A). Direct comparison of the morphologies of PTTH and EH neurons showed that the dendrites of EH neurons intermingled with the medial dendritic arborizations of PTTH neurons (Fig. 1B, C). Further confirmation was established with GFP reconstitution across synaptic partners (GRASP) [34, 35]. We found significant recombinant GFP signals only in the region of overlapping dendrites, while no signal was seen in the controls (Fig. 1D, F). It is noteworthy that no GRASP signal was found in the ring gland where the axonal termini of PTTH and EH neurons are located (Fig. 1D). Thus, there might be a physical interaction between the dendrites of PTTH and EH neurons.

Next, we combined Ca^{2+} imaging with optogenetics to further confirm the existence of a functional connection between EH and PTTH neurons. We found that, as expected, exciting PTTH neurons induced a robust increase in fluorescence in EH neurons. The peak response of a >100% increase was reached within 4 s of the onset of red light stimulation (Fig. 1G, H). Interestingly, optogenetic activation of EH neurons inhibited PTTH neurons by >40% as measured by fluorescence intensity (Fig. 1I, J). These results supported the existence of dendrodendritic synapses between PTTH and EH neurons; recurrent inhibition is commonly seen in dendrodendritic interactions [37, 38]. Taken together, our results suggested that EH neurons receive visual input *via* PTTH neurons.

EH Neurons Mediate Deceleration in Larval Light-Avoidance

We then asked if EH neurons are required for larval light-avoidance. Larvae expressing *UAS-TNTG* [38], or *UAS-dORKΔC* [40] with *EH-Gal4* [31] exhibited impaired phototaxis, and this effect was reversed by the introduction of *elav-Gal80* (Fig. 2A). This finding was confirmed using *R28E02-Gal4*, which labeled the same two neurons as *EH-Gal4* (Fig. S3). A possible developmental effect of inhibition could be excluded using the temporal and regional gene expression targeting (TARGET) system [40] in which *Tub-Gal80^{ts}* was combined with *EH-Gal4* and *UAS-dORKΔC*. After being heat-shocked at 32°C for 12 h to allow instant expression of *dORKΔC* and thus inhibition of EH neurons; mid-late third-instar larvae that had been raised at 18°C showed no light-avoidance. Sibling larvae that did not receive this heat-shock treatment demonstrated normal light avoidance (Fig. 2B). Furthermore, hyperactivating EH neurons by expressing the depolarizing Na^+ channel NaChBac [41] enhanced the larval preference for darkness over light (Fig. S3D). Together, these results suggested that EH neurons are required for larval light-avoidance.

To determine whether EH neurons are required for the light-induced deceleration and the head casting, we tested the light-avoidance using a light-spot assay during which detailed larval behavior was recorded [19]. Compared with the control parental lines, the degree of the light-induced head casting was reduced when the EH neurons were blocked with *UAS-TNTG* (Fig. 2C). This was to be expected as defects in head casting and turning behavior appeared to be directly linked to the loss of light-avoidance. Notably, the minimal speed after light-induced deceleration was significantly higher in the larvae with inhibited EH neurons than in control lines (Fig. 2D). The higher minimal speed was not due to increased locomotor speed because that of the experimental line was not higher than that of the control lines. Note that the locomotor speed in all three lines was >1 mm/s, the normal speed of locomotion (Fig. S2). Thus, EH neurons appear to be

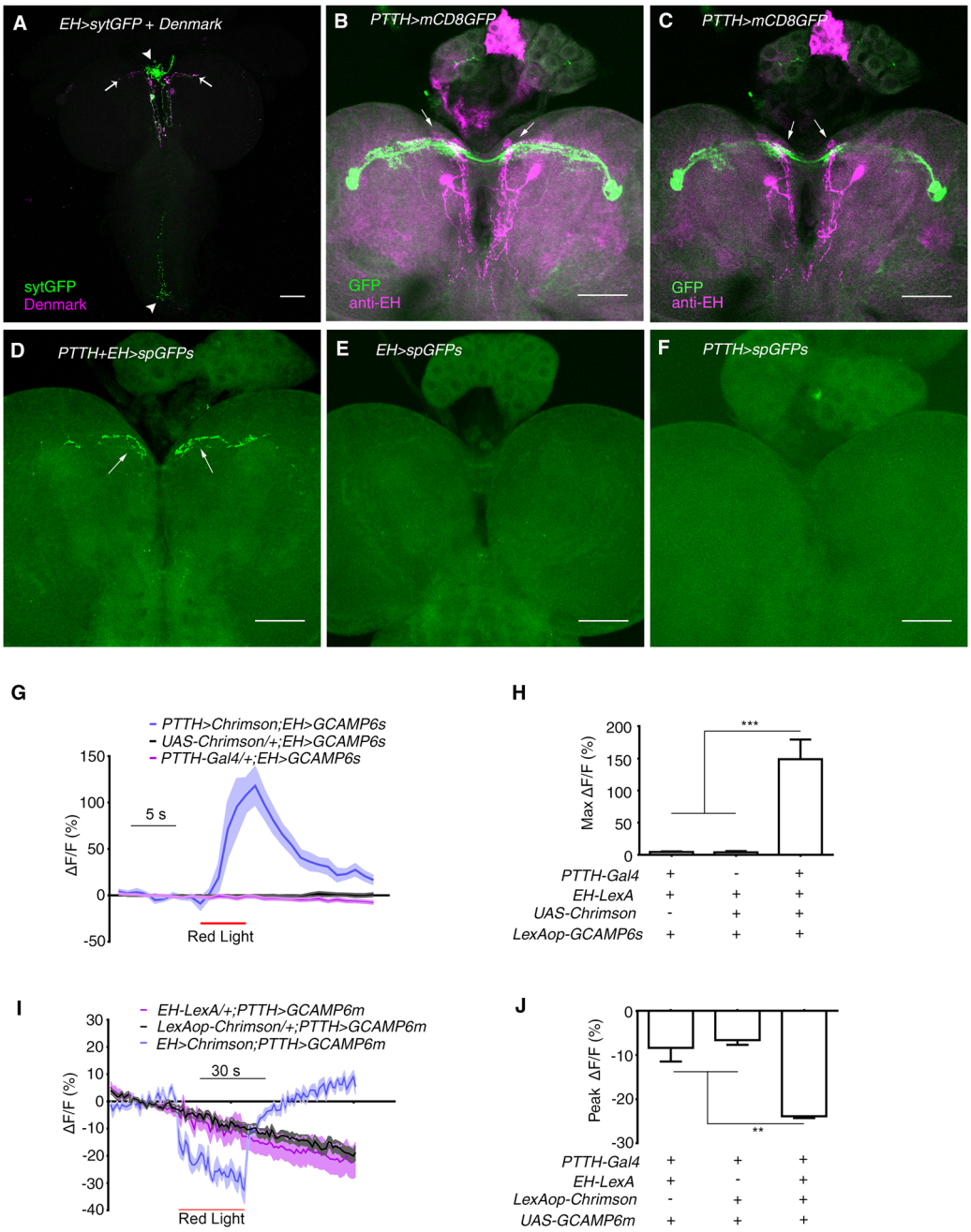

Fig. 1 EH neurons receive visual input from PTTH neurons. **A** Expression of the pre- and post-synaptic markers sytGFP and Denmark, respectively, in EH neurons using *EH-Gal4* (green, sytGFP; magenta, Denmark; arrows indicate dendrites; arrowheads indicate axonal termini). **B** Stacked image of co-staining of *PTTH-Gal4* and anti-EH in larval central brain (green, *PTTH-Gal4* marked by GFP; magenta, anti-EH signal; arrows indicate co-localization). **C** Single-layer view of (**B**). Arrows indicate co-localization. **D**–**F** GRASP between PTTH and EH neurons. **D** The GFP signal occurred where the dendrites of PTTH and EH neurons overlap (arrows). **E**, **F** GRASP control in which split GFP expression was driven by *EH-LexA* (**E**) or *PTTH-Gal4* (**F**). **G** Optogenetic activation of PTTH neurons stimulated a Ca^{2+} response in EH neurons (n = 13 for *PTTH-Gal4/+*; *EH > GCAMP6s*, 10 for *UAS-Chrimson/+*; *EH > GCAMP6s*, and 8 for *PTTH > Chrimson*; *EH > GCAMP6s*. **H** Quantification of the peak Ca^{2+} response in (**G**) (***$P < 0.001$). **I** Optogenetic activation of EH neurons inhibited the Ca^{2+} signal in PTTH neurons (n = 12 for *EH-LexA/+*; *PTTH > GCAMP6m*, 16 for *LexAop-Chrimson/+*; *PTTH > GCAMP6m*, and 5 for *EH > Chrimson*; *PTTH > GCAM6m*. **J** Quantification of peak Ca^{2+} response during red light stimulation in (**I**) (**$P < 0.01$). Red lines in (**G**) and (**I**), periods of optogenetic stimulation. Scale bars, 50 μm in (**A**–**F**). One-way ANOVA followed by *post hoc Tukey's* multiple comparison test was used for (**H**) and (**J**).

required for light-evoked deceleration, in addition to light-induced head casting in light-avoidance.

To verify that EH neurons indeed receive input from larval "photoreceptors" – the BOs – we combined

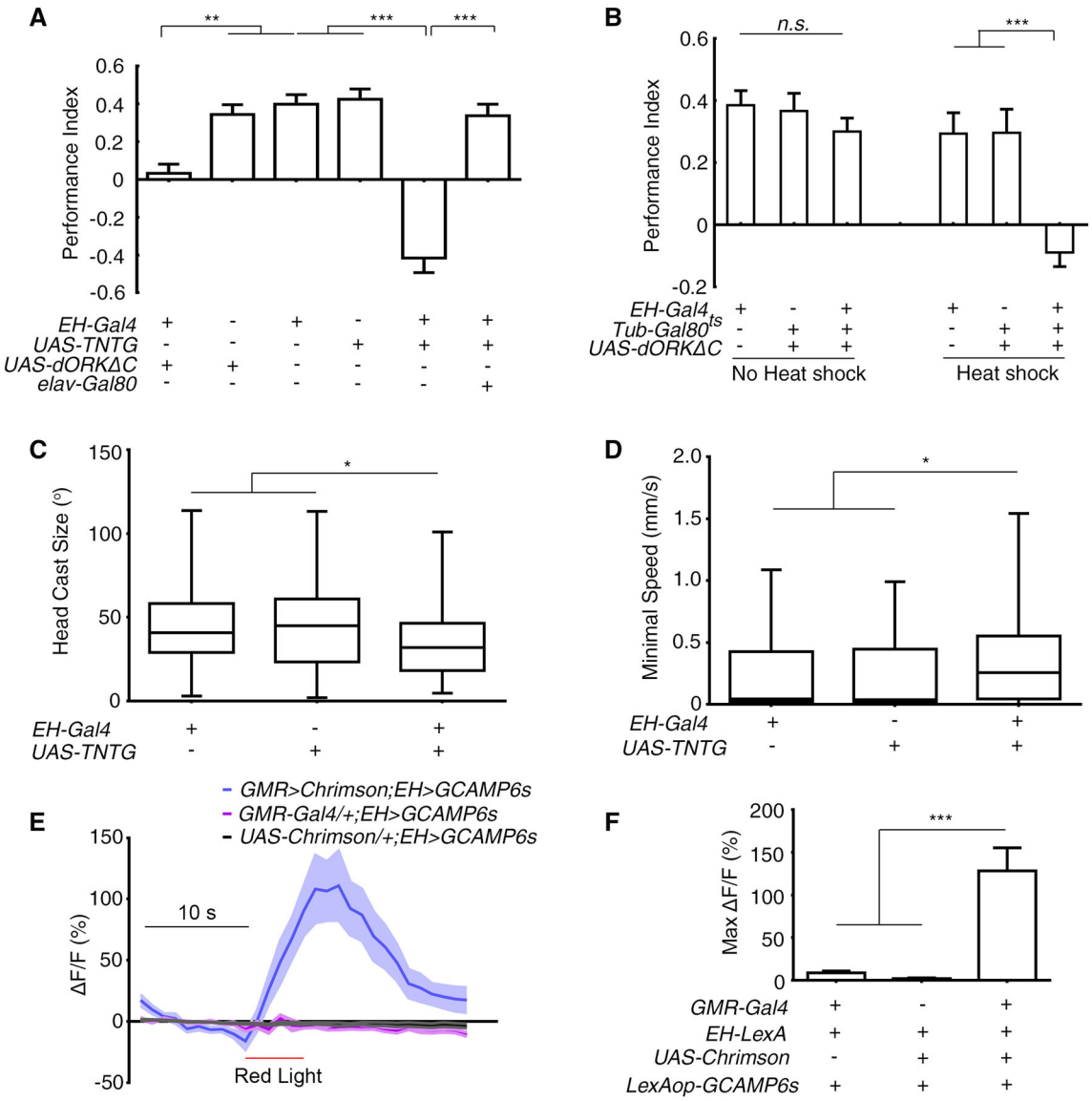

Fig. 2 Larval EH neurons were part of the visual pathway that commanded the deceleration in light avoidance. **A** Inhibiting EH neurons abolished the preference for darkness (**$P < 0.01$, ***$P < 0.001$; n = 19, 16, 17, 16, 19, and 19 from left to right). **B** Acute inhibition of EH neurons abolished the preference for darkness (Heat shock, with restrictive temperature; No heat shock, with permissive temperature; ***$P < 0.001$, *n.s.*, not significant; n = 17 for all groups). **C**, **D** Inhibiting EH neurons decreased the degree of head casting in response to light-spot entry (**C**) and increased the minimal speed after light-evoked deceleration (**D**) (*$P < 0.05$, n = 99, 67, and 70 in (**C**) and n = 100, 69, and 72 in (**D**) for *EH-Gal4/+*, *UAS-TNTG/+*, and *EH > TNTG*, respectively). **E** Ca^{2+} imaging of cell bodies of EH neurons expressing GCAMP6s in response to optogenetic activation of *GMR-Gal4*-labeled photoreceptor neurons (n = 11 for *GMR > Chrimson*; *EH > GCAMP6s*, 9 for *GMR-Gal4/+*; *EH > GCAMP6s*, and 10 for *UAS-Chrimson/+*; *EH > GCAMP6s*. **F** Quantification of peak Ca^{2+} imaging responses in (**E**) (***$P < 0.001$). One-way ANOVA followed by *post hoc Tukey's* multiple comparison test was used for (**A**, **B**) and (**F**); the *Kruskal-Wallis* test followed by *post hoc Dunn's* multiple comparison test was used for (**C**, **D**).

optogenetics with Ca^{2+} imaging to directly activate their photoreceptors and record the response of EH neurons [42]. Larvae with *UAS-Chrimson* expressed in larval photoreceptors with *GMR-Gal4* and GCAMP6 [43] expressed in EH neurons were cultured on food supplied with all-trans-retinal. Upon stimulation of the photoreceptors by red light, we recorded an immediate and strong Ca^{2+} response of ~100% increase in fluorescence intensity in the cell bodies (Fig. 2E, F).

Taken together, EH neurons are part of the larval visual pathway required for the light-evoked deceleration. These neurons might indirectly affect head casting by regulating deceleration.

EH Neurons Innervate Tdc2 Motor Neurons in Larval Light-Avoidance

As the axons of EH neurons project through the larval VNC, we examined whether they directly innervate motor neurons that are involved in processing light-avoidance behavior. Close proximity was easily detected at the level of single confocal sections when motor-neuron-specific *D42-Gal4* was counterstained with anti-EH (data not shown). As *D42-Gal4* was comprehensively expressed, we asked specifically which motor neurons were innervated by EH neurons. We tested *Tdc2-Gal4*-labeled motor neurons [44] by comparing *Tdc2-Gal4* [45] with anti-EH in the larval nervous system. In addition to sporadic overlapping in the brain, the anti-EH signal overlapped well with the *Tdc2-Gal4* signal in abdominal segments of the VNC (Fig. 3A, B). We next used GRASP to confirm the physical interaction between EH neurons and Tdc2 motor neurons in the VNC. Again, we observed a GRASP signal between EH neurons and *Tdc2-Gal4*-labeled neurons in the VNC (Fig. 3C–E). Thus, EH neurons directly innervate Tdc2 motor neurons.

We further confirmed the EH-Tdc2 neuronal interaction using a combination of optogenetics and Ca^{2+} imaging. Upon stimulation of EH neurons with 620-nm light, we observed a >50% increase in fluorescence intensity within 5 s in the avm3 and avm7 clusters of Tdc2 neuron cell bodies in abdominal segments (Fig. 3F, Fig. S4). The Ca^{2+} response was not significant in Tdc2 neurons in other abdominal segments. Thus, we confirmed that EH neurons innervate *Tdc2-Gal4* neurons, at least those in the avm3 and avm7 clusters.

Tdc2 Motor Neurons Mediate Deceleration in Larval Light-Avoidance

Although we had determined that *Tdc2-Gal4*-labeled neurons were targeted by EH neurons, whether larval Tdc2 motor neurons were required for the light-evoked deceleration and light-avoidance was unclear. Thus, we

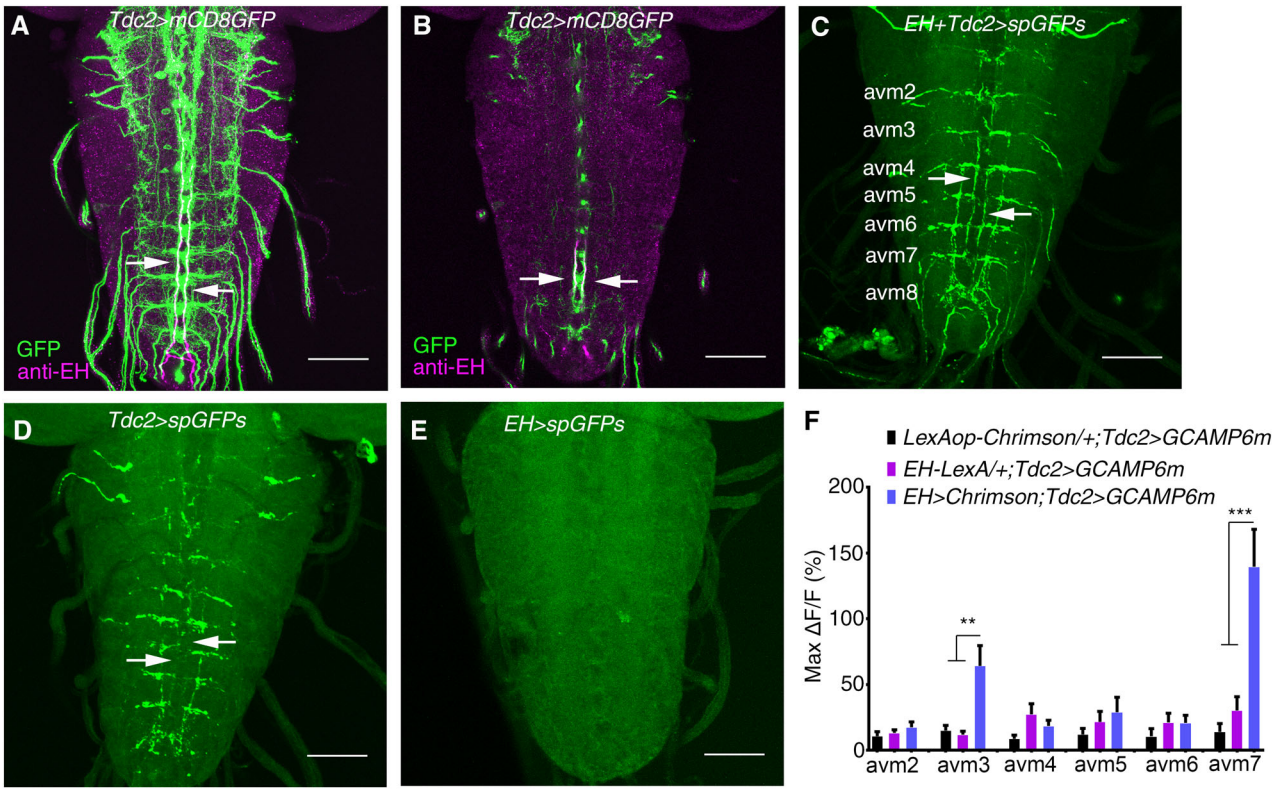

Fig. 3 EH neurons innervate Tdc2 motor neurons. **A** Stacked image of co-staining of *Tdc2-Gal4* marked by GFP and anti-EH in the larval VNC (green, GFP signal; magenta, anti-EH signal; arrows indicate co-localization. **B** Single layer view of (**A**). Arrows indicate co-localization. **C–E** GRASP between EH neurons and Tdc2 motor neurons (**C**). The GFP signal is seen where the axonal termini of EH neurons and the dendrites of Tdc2 motor neurons overlap, as indicated by arrows. **D**, **E** GRASP control in which split GFP expression was driven by *Tdc2-Gal4* (**D**) and *EH-LexA* (**E**). No GFP signal for GRASP was seen (arrows). **F** Statistics of the peak Ca^{2+} response in cell bodies of Tdc2 motor neurons upon optogenetic activation of EH neurons (**$P < 0.01$, ***$P < 0.001$, one-way ANOVA and post hoc *Tukey's* multiple comparison test; no other significant differences between the experimental and control groups. See Fig. S4 for details. Scale bars, 50 μm in **A–E**.

blocked *Tdc2-Gal4*-labeled neurons by expressing *TNTG* and *dORKΔC*. Larvae with inhibited *Tdc2-Gal4* neurons lost light-avoidance (Fig. 4A). Introduction of VNC-specific *tsh-Gal80* [46] that prevented *Tdc2-Gal4* expression in the VNC restored normal light-avoidance, suggesting that the Tdc2 motor neurons in the VNC are required for the light preference (Fig. 4A). When the TARGET system was used to exclude possible developmental effects, light-avoidance in larvae subjected to 12 h of 32°C heat shock was abolished, while the control larvae raised at 18°C throughout had intact light-avoidance (Fig. 4B). Thus, Tdc2 motor neurons are required for normal light-avoidance. We next conducted the light-spot assay in larvae in which Tdc2 neurons were blocked with *TNTG*. These larvae demonstrated a lesser degree of head casting when encountering light (Fig. 4C). However, their minimum speed after light-induced deceleration was not significantly greater than that in the parental controls (Fig. 4D). Considering that the inhibition of Tdc2 motor neurons led to slower locomotion in free movement (Fig. S2) [44], the lack of a change in minimal speed after deceleration might reflect less deceleration in response to light stimulation. Thus, inhibiting Tdc2 neurons appeared to undermine the light-induced deceleration and head casting.

Activation of PET Pathway Neurons Induced Deceleration

We attempted to verify the function of PET pathway neurons in deceleration by activating them artificially using optogenetics. We drove the expression of *UAS-Chrimson* [47] with *PTTH-Gal4*, *EH-Gal4*, and *Tdc2-Gal4*. Upon stimulation with 620-nm light, larvae raised on food containing all-trans-retinal showed more speed reduction than controls, though the deceleration response was mild (Fig. 5A, B for PTTH neurons, 5C, D for EH neurons, 5E, F for Tdc2 motor neurons, Movie S2–5). This finding was confirmed using *NP423-Gal4* and *R28E02-Gal4* that respectively labeled PTTH neurons and EH neurons (Fig. S3E–L and Fig. S5). It should be noted that head

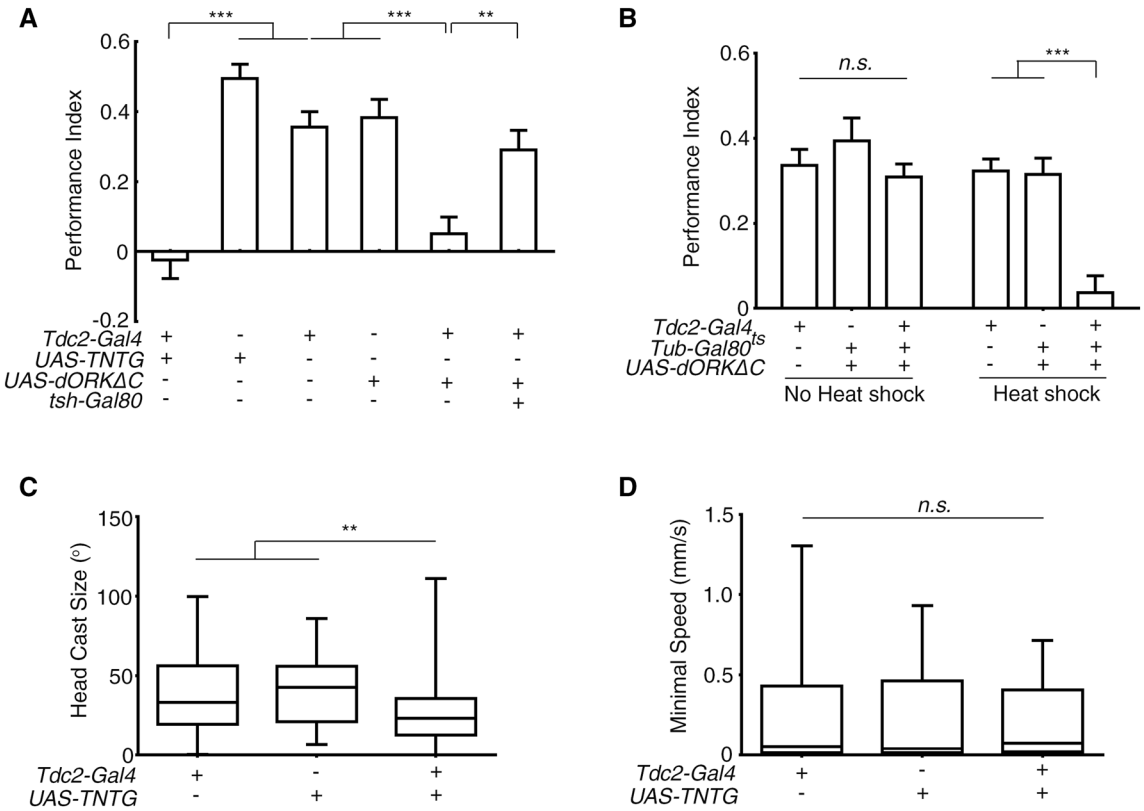

Fig. 4 Tdc2 motor neurons mediated light-induced deceleration. **A** Inhibiting Tdc2 motor neurons abolished larval preference for darkness (**$P < 0.01$, ***$P < 0.001$; n = 22, 23, 17, 19, 23, and 23 from left to right). **B** Acute inhibition of Tdc2 neurons abolished the preference for darkness (Heat shock, with restrictive temperature; No heat shock, with permissive temperature; ***$P < 0.001$, *n.s.*, not significant; n = 29, 19, 47, 15, 19, and 28 from left to right). **C**, **D** Effect of inhibiting Tdc2 neurons on larval head casting and deceleration in response to light-spot entry. **C** The degree of head casting was decreased. **D** The minimum speed after deceleration did not differ from controls (**$P < 0.01$, *n.s.*, not significant; n = 81, 52, and 92 in (**C**) and 82, 53, and 96 in (**D**) for *Tdc2-Gal4*, *UAS-TNTG/+* and *Tdc2 > TNTG*, respectively). One-way ANOVA followed by post hoc *Tukey's* multiple comparison test was used for **A** and **B**. *Kruskal-Wallis* test followed by post hoc *Dunn's* multiple comparison test was used for **C** and **D**.

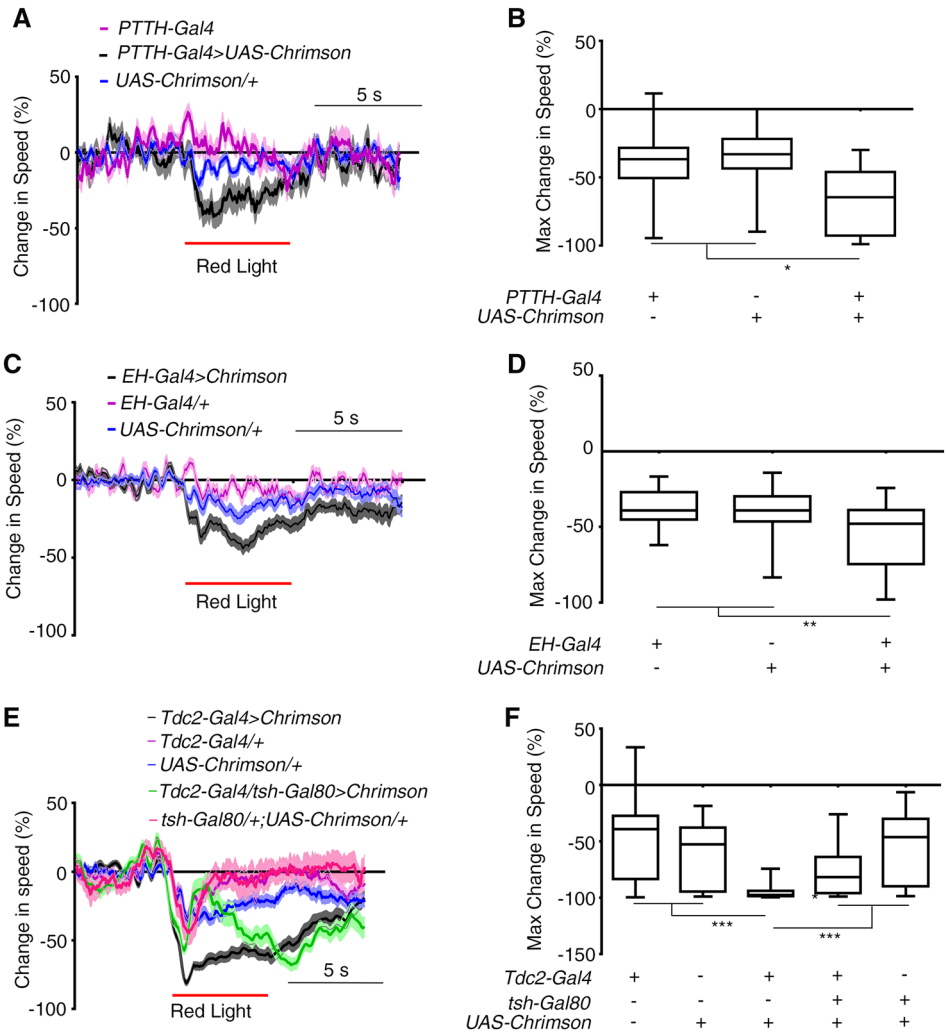

Fig. 5 Optogenetic activation of PET pathway neurons induced deceleration. **A**, **B** Optogenetic activation of PTTH neurons using *PTTH-Gal4* led to strong deceleration. **A** Time curves of percentage change in larval tail speed. **B** Maximum decrease in tail speed within 2 s after optogenetic activation of PTTH neurons (n = 15, 23, and 20 for *PTTH-Gal4* > *Chrimson*, *UAS-Chrimson/+*, and *PTTH-Gal4*, respectively; red line, period of optogenetic stimulation). **C-D** Optogenetic activation of EH neurons using *EH-Gal4* led to a deceleration in larval locomotion. **C** Time curves of percentage change in larval tail speed. **D** Maximum decrease in tail speed within 2 s after optogenetic activation. n = 40, 37, and 29 for *EH-Gal4* > *Chrimson*, *UAS-Chrimson/+*, and *EH-Gal4/+*, respectively. **E**, **F** Optogenetic activation of Tdc2 neurons led to strong deceleration. Time curves of percentage change in larval tail speed (**E**). Maximum decrease in tail speed within 2 s of optogenetic activation of Tdc2 neurons labeled with *Tdc2-Gal4* (**F**) (n = 44, 45, 43, 37, and 15 for *Tdc2-Gal4*, *UAS-Chrimson*, *Tdc2-Gal4* > *Chrimson*, *Tdc2-Gal4/tsh-Gal80* > *Chrimson*, and *tsh-Gal80/+*; *UAS-Chrimson/+*, respectively; red lines, period of optogenetic stimulation in (**A**), (**C**) and (**E**)). $^{*}P < 0.05$, $^{**}P < 0.01$, $^{***}P < 0.001$, *Kruskal-Wallis* test followed by post hoc *Dunn's* multiple comparison test was used for (**B**), (**D**), and (**F**).

casting was not always seen after deceleration, suggesting that the activation of PET pathway neurons specifically induces deceleration.

Discussion

In this study, we found that larvae need to decelerate before making a head cast in light-avoidance. This represents an additional stage of deceleration between the locomotion and head casting that have received the most attention in studies of larval avoidance behavior. The results showed that the light-induced deceleration response is mediated by the PET pathway and facilitates subsequent head casting in larval light-avoidance behavior.

PET pathway neurons can inhibit locomotion in different ways. First, Tdc2 motor neurons may use tyramine as a neurotransmitter, which can play an inhibitory role by inhibiting muscle cells and thus stopping larval locomotion [48, 49]. Another possibility is that a light stimulus may disturb the regular firing of Tdc2 motor neurons or their downstream neurons required for the normal rhythm of

locomotion. Because motor neurons or pre-motor neurons need to fire in a specific sequence for coordinated locomotion [45, 50–52], disturbing the sequence may be a natural way of reducing locomotor speed. If Tdc2 motor neurons themselves do not produce firing sequences to drive periodic locomotion, they may regulate locomotor central pattern generator (CPG) neurons in the larval VNC, for example, *via* gap junctions between motor neurons and premotor neurons [52–54]. In either case, activating Tdc2 neurons in a larva by an external stimulus can interfere with its locomotor rhythm and reduce its crawling speed.

Most stop responses in previous reports, such as the gentle touch in *Drosophila* larvae, touch in tadpoles, and the stop mediated by reticulospinal V2a neurons in mice, appear to result in a full stop with no subsequent turning behavior [15–17]. The PET-mediated light-induced deceleration response seems to be an emergent stop response that is generally followed by a head cast. As the head cast is actually initiated during the process of deceleration, deceleration can be considered as a preparatory stage for head casting.

In the PET pathway, the long axonal projections of EH neurons resemble those of the reticulospinal neurons that command stop responses in vertebrates [16–18]. These neurons also have cell bodies and dendrites located in the brain to receive input from higher order neurons, while sending long axonal projections to innervate locomotor CPG neurons in the spinal cord and produce a stop response. It is likely that sensory stimulus-induced deceleration responses in vertebrate avoidance behavior are mediated by neuronal pathways similar to the PET pathway.

Therefore, in support of the hypothesis that there is a separate neural pathway for controlling deceleration prior to avoiding danger, the discovery of the PET pathway gives a new insight into survival-critical avoidance behaviors of animals in general.

Acknowledgements We thank Mathieu Louis for sharing free SOS codes; Michael O'Cornor for *PTTH-Gal4*; Berni Jimena for *tsh-Gal80*; and Xiaohui Zhang, Chao Tong, Xiaohang Yang, Liming Wang, and Yijun Liu for sharing reagents and valuable discussions. We also thank the Bloomington *Drosophila* Stock Center and Qinghua *Drosophila* Stock Center for providing the fly stocks, and the core facilities of Zhejiang University School of Medicine for technical support. This work was supported by grants from the National Basic Research Development Program of China (973 Program, 2013CB945603), the National Natural Science Foundation of China (31070944, 31271147, 31471063, 31671074, and 61572433), the Natural Science Foundation of Zhejiang Province, China (LR13C090001 and LZ14F020002), and the Fundamental Research Funds for the Central Universities, China (2017FZA7003).

Compliance with Ethical Standards

Conflict of interest The authors declare no competing interest.

References

1. Bidaye SS, Machacek C, Wu Y, Dickson BJ. Neuronal control of Drosophila walking direction. Science 2014, 344: 97–101.
2. Sen R, Wu M, Branson K, Robie A, Rubin GM, Dickson BJ. Moonwalker Descending Neurons Mediate Visually Evoked Retreat in Drosophila. Curr Biol 2017, 27: 766–771.
3. von Reyn CR, Breads P, Peek MY, Zheng GZ, Williamson WR, Yee AL, *et al.* A spike-timing mechanism for action selection. Nat Neurosci 2014, 17: 962–970.
4. von Reyn CR, Nern A, Williamson WR, Breads P, Wu M, Namiki S, *et al.* Feature Integration Drives Probabilistic Behavior in the Drosophila Escape Response. Neuron 2017, 94: 1190–1204 e1196.
5. Wu M, Nern A, Williamson WR, Morimoto MM, Reiser MB, Card GM, *et al.* Visual projection neurons in the Drosophila lobula link feature detection to distinct behavioral programs. Elife 2016, 5.
6. Gomez-Marin A, Stephens GJ, Louis M. Active sampling and decision making in Drosophila chemotaxis. Nat Commun 2011, 2: 441.
7. Lahiri S, Shen K, Klein M, Tang A, Kane E, Gershow M, *et al.* Two alternating motor programs drive navigation in Drosophila larva. PLoS One 2011, 6: e23180.
8. Kane EA, Gershow M, Afonso B, Larderet I, Klein M, Carter AR, *et al.* Sensorimotor structure of Drosophila larva phototaxis. Proc Natl Acad Sci U S A 2013, 110: E3868–3877.
9. Tastekin I, Riedl J, Schilling-Kurz V, Gomez-Marin A, Truman JW, Louis M. Role of the subesophageal zone in sensorimotor control of orientation in Drosophila larva. Curr Biol 2015, 25: 1448–1460.
10. Grillner S. Biological pattern generation: the cellular and computational logic of networks in motion. Neuron 2006, 52: 751–766.
11. Grillner S, Robertson B. The basal ganglia downstream control of brainstem motor centres-an evolutionarily conserved strategy. Curr Opin Neurobiol 2015, 33: 47–52.
12. Kiehn O. Decoding the organization of spinal circuits that control locomotion. Nat Rev Neurosci 2016, 17: 224–238.
13. Ryczko D, Auclair F, Cabelguen JM, Dubuc R. The mesencephalic locomotor region sends a bilateral glutamatergic drive to hindbrain reticulospinal neurons in a tetrapod. J Comp Neurol 2016, 524: 1361–1383.
14. Caggiano V, Leiras R, Goni-Erro H, Masini D, Bellardita C, Bouvier J, *et al.* Midbrain circuits that set locomotor speed and gait selection. Nature 2018, 553: 455–460.
15. Kernan M, Cowan D, Zuker C. Genetic dissection of mechanosensory transduction: mechanoreception-defective mutations of Drosophila. Neuron 1994, 12: 1195–1206.
16. Perrins R, Walford A, Roberts A. Sensory activation and role of inhibitory reticulospinal neurons that stop swimming in hatchling frog tadpoles. J Neurosci 2002, 22: 4229–4240.
17. Bouvier J, Caggiano V, Leiras R, Caldeira V, Bellardita C, Balueva K, *et al.* Descending Command Neurons in the Brainstem that Halt Locomotion. Cell 2015, 163: 1191–1203.
18. Juvin L, Gratsch S, Trillaud-Doppia E, Gariepy JF, Buschges A, Dubuc R. A Specific Population of Reticulospinal Neurons Controls the Termination of Locomotion. Cell Rep 2016, 15: 2377–2386.
19. Zhao W, Gong C, Ouyang Z, Wang P, Wang J, Zhou P, *et al.* Turns with multiple and single head cast mediate Drosophila larval light avoidance. PLoS One 2017, 12: e0181193.
20. Gershow M, Berck M, Mathew D, Luo L, Kane EA, Carlson JR, *et al.* Controlling airborne cues to study small animal navigation. Nat Methods 2012, 9: 290–296.

21. Xiang Y, Yuan Q, Vogt N, Looger LL, Jan LY, Jan YN. Light-avoidance-mediating photoreceptors tile the Drosophila larval body wall. Nature 2010, 468: 921–926.
22. Mazzoni EO, Desplan C, Blau J. Circadian pacemaker neurons transmit and modulate visual information to control a rapid behavioral response. Neuron 2005, 45: 293–300.
23. Collins B, Kane EA, Reeves DC, Akabas MH, Blau J. Balance of activity between LN(v)s and glutamatergic dorsal clock neurons promotes robust circadian rhythms in Drosophila. Neuron 2012, 74: 706–718.
24. Keene AC, Sprecher SG. Seeing the light: photobehavior in fruit fly larvae. Trends Neurosci 2012, 35: 104–110.
25. Gong Z, Liu J, Guo C, Zhou Y, Teng Y, Liu L. Two pairs of neurons in the central brain control Drosophila innate light preference. Science 2010, 330: 499–502.
26. Yamanaka N, Romero NM, Martin FA, Rewitz KF, Sun M, O'Connor MB, *et al.* Neuroendocrine control of Drosophila larval light preference. Science 2013, 341: 1113–1116.
27. Selcho M, Millan C, Palacios-Munoz A, Ruf F, Ubillo L, Chen J, *et al.* Central and peripheral clocks are coupled by a neuropeptide pathway in Drosophila. Nat Commun 2017, 8: 15563.
28. McBrayer Z, Ono H, Shimell M, Parvy JP, Beckstead RB, Warren JT, *et al.* Prothoracicotropic hormone regulates developmental timing and body size in Drosophila. Dev Cell 2007, 13: 857–871.
29. Hicheur H, Vieilledent S, Richardson MJ, Flash T, Berthoz A. Velocity and curvature in human locomotion along complex curved paths: a comparison with hand movements. Exp Brain Res 2005, 162: 145–154.
30. Zago M, Lacquaniti F, Gomez-Marin A. The speed-curvature power law in Drosophila larval locomotion. Biol Lett 2016, 12.
31. McNabb SL, Baker JD, Agapite J, Steller H, Riddiford LM, Truman JW. Disruption of a behavioral sequence by targeted death of peptidergic neurons in Drosophila. Neuron 1997, 19: 813–823.
32. Zhang YQ, Rodesch CK, Broadie K. Living synaptic vesicle marker: synaptotagmin-GFP. Genesis 2002, 34: 142–145.
33. Nicolai LJ, Ramaekers A, Raemaekers T, Drozdzecki A, Mauss AS, Yan J, *et al.* Genetically encoded dendritic marker sheds light on neuronal connectivity in Drosophila. Proc Natl Acad Sci U S A 2010, 107: 20553–20558.
34. Feinberg EH, Vanhoven MK, Bendesky A, Wang G, Fetter RD, Shen K, *et al.* GFP Reconstitution Across Synaptic Partners (GRASP) defines cell contacts and synapses in living nervous systems. Neuron 2008, 57: 353–363.
35. Gordon MD, Scott K. Motor control in a Drosophila taste circuit. Neuron 2009, 61: 373–384.
36. Shepherd GM. Symposium overview and historical perspective: dendrodendritic synapses: past, present, and future. Ann N Y Acad Sci 2009, 1170: 215–223.
37. Urban NN, Arevian AC. Computing with dendrodendritic synapses in the olfactory bulb. Ann N Y Acad Sci 2009, 1170: 264–269.
38. Sweeney ST, Broadie K, Keane J, Niemann H, O'Kane CJ. Targeted expression of tetanus toxin light chain in Drosophila specifically eliminates synaptic transmission and causes behavioral defects. Neuron 1995, 14: 341–351.
39. Nitabach MN, Blau J, Holmes TC. Electrical silencing of Drosophila pacemaker neurons stops the free-running circadian clock. Cell 2002, 109: 485–495.
40. McGuire SE, Roman G, Davis RL. Gene expression systems in Drosophila: a synthesis of time and space. Trends Genet 2004, 20: 384–391.
41. Nitabach MN, Wu Y, Sheeba V, Lemon WC, Strumbos J, Zelensky PK, *et al.* Electrical hyperexcitation of lateral ventral pacemaker neurons desynchronizes downstream circadian oscillators in the fly circadian circuit and induces multiple behavioral periods. J Neurosci 2006, 26: 479–489.
42. Akerboom J, Carreras Calderon N, Tian L, Wabnig S, Prigge M, Tolo J, *et al.* Genetically encoded calcium indicators for multi-color neural activity imaging and combination with optogenetics. Front Mol Neurosci 2013, 6: 2.
43. Chen TW, Wardill TJ, Sun Y, Pulver SR, Renninger SL, Baohan A, *et al.* Ultrasensitive fluorescent proteins for imaging neuronal activity. Nature 2013, 499: 295–300.
44. Selcho M, Pauls D, El Jundi B, Stocker RF, Thum AS. The role of octopamine and tyramine in Drosophila larval locomotion. J Comp Neurol 2012, 520: 3764–3785.
45. Yue Fei, Dikai Zhu. Repeated failure in reward pursuit alters innate drosophila larval behaviors. Neurosci Bull 2018, 34(6):901–911.
46. Berni J, Pulver SR, Griffith LC, Bate M. Autonomous circuitry for substrate exploration in freely moving Drosophila larvae. Curr Biol 2012, 22: 1861–1870.
47. Klapoetke NC, Murata Y, Kim SS, Pulver SR, Birdsey-Benson A, Cho YK, *et al.* Independent optical excitation of distinct neural populations. Nat Methods 2014, 11: 338–346.
48. Saraswati S, Fox LE, Soll DR, Wu CF. Tyramine and octopamine have opposite effects on the locomotion of Drosophila larvae. J Neurobiol 2004, 58: 425–441.
49. Fox LE, Soll DR, Wu CF. Coordination and modulation of locomotion pattern generators in Drosophila larvae: effects of altered biogenic amine levels by the tyramine beta hydroxlyase mutation. J Neurosci 2006, 26: 1486–1498.
50. Kohsaka H, Takasu E, Morimoto T, Nose A. A group of segmental premotor interneurons regulates the speed of axial locomotion in Drosophila larvae. Curr Biol 2014, 24: 2632–2642.
51. Itakura Y, Kohsaka H, Ohyama T, Zlatic M, Pulver SR, Nose A. Identification of Inhibitory Premotor Interneurons Activated at a Late Phase in a Motor Cycle during Drosophila Larval Locomotion. PLoS One 2015, 10: e0136660.
52. Matsunaga T, Kohsaka H, Nose A. Gap Junction-Mediated Signaling from Motor Neurons Regulates Motor Generation in the Central Circuits of Larval Drosophila. J Neurosci 2017, 37: 2045–2060.
53. Prendergast A, Wyart C. Locomotion: Electrical Coupling of Motor and Premotor Neurons. Curr Biol 2016, 26: R235–237.
54. Song J, Ampatzis K, Bjornfors ER, El Manira A. Motor neurons control locomotor circuit function retrogradely via gap junctions. Nature 2016, 529: 399–402.